NACA

RESEARCH MEMORANDUM

INVESTIGATION OF MECHANISMS OF BLADE FAILURE OF

FORGED HASTELLOY B AND CAST STELLITE 21

TURBINE BLADES IN TURBOJET ENGINE
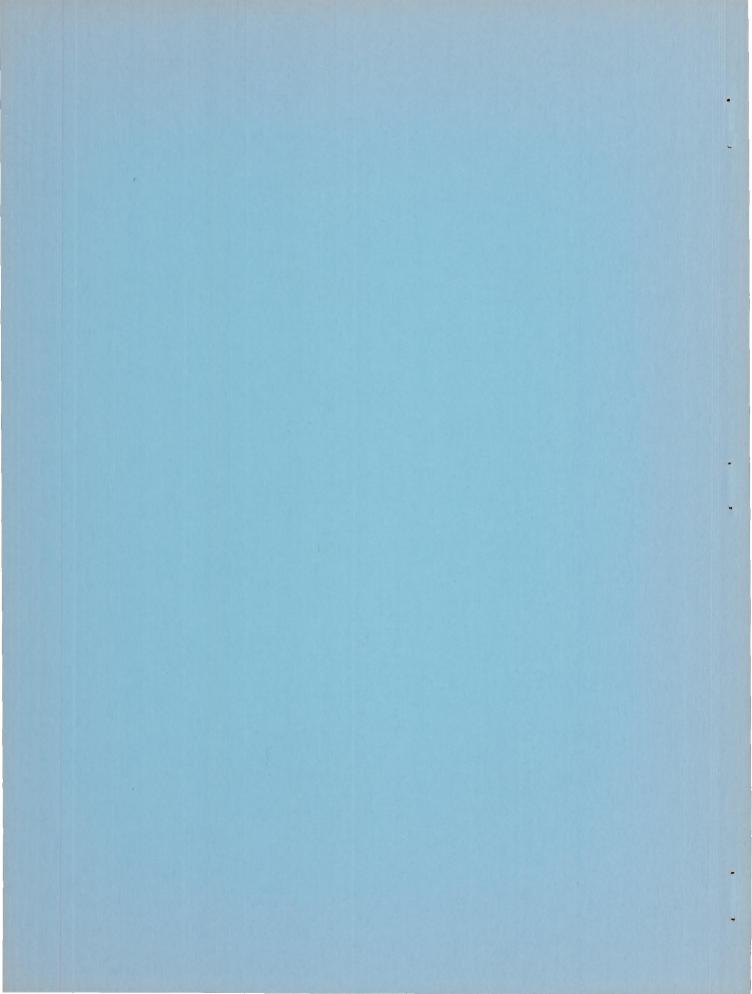
By C. Yaker, C. F. Robards, and F. B. Garrett

Lewis Flight Propulsion Laboratory
Cleveland, Ohio

NATIONAL ADVISORY COMMITTEE
FOR AERONAUTICS
WASHINGTON

NATIONAL ADVISORY COMMITTEE FOR AERONAUTICS

RESEARCH MEMORANDUM

INVESTIGATION OF MECHANISMS OF BLADE FAILURE OF

FORGED HASTELLOY B AND CAST STELLITE 21

TURBINE BLADES IN TURBOJET ENGINE

By C. Yaker, C. F. Robards, and F. B. Garrett

· SUMMARY

An investigation was conducted to determine the mechanisms of
failure of turbine blades of Hastelloy B, a forged nickel-base alloy,
and Stellite 21, a precision-cast cobalt-base alloy, when operated
in a J33-9 turbojet engine. The blades were alternately spaced in a
16-25-6 alloy rotor and subjected to simulated service operation con-
sisting of 20-minute cycles (15 min at rated speed and approximately
5 min at idle). The engine conditions at rated speed were 11,500 rpm
and a gas temperature of 1250° F at the exhaust-cone outlet. For these
operating conditions, the estimated maximum blade temperature in the
normal zone of failure was 1500° F and the centrifugal stress in this
zone was 25,000 pounds per square inch for the Hastelloy B and
21,000 pounds per square inch for the Stellite 21 blades.

The results of stress-rupture tests on specimens cut from blades
indicated that the minimum blade life at rated speed should be
10.3 hours for Hastelloy B and 21 hours for Stellite 21. The first
Hastelloy B blade failed after 14.25 hours (57 cycles) at rated speed;
the first Stellite 21 blade failed after 16.75 hours (67 cycles).
Both of these failures originated at the trailing edges of the blades
and were probably the result of excessive vibratory stresses. Inter-
crystalline cracking of the stress-rupture type was detected in both
alloys after 16.75 hours (67 cycles) of operation. Additional failures
of Hastelloy B blades occurred after 18.47 hours ($<$ 74 cycles) and
28.75 hours (115 cycles) at rated speed as a result of the propagation
of the previously formed intercrystalline cracks. These failures
progressed by both fatigue and stress-rupture mechanisms. After
28.75 hours of operation, all but three of the original 27 Hastelloy B
blades had either failed or contained stress-rupture-type cracks.
No additional Stellite 21 failures occurred up to 28.75 hours
(115 cycles) at rated conditions except two blades fractured by impact

with the fractured half of a Hastelloy B blade. After 28.75 hours of
operation, stress-rupture-type cracks had formed in four of the
original Stellite 21 blades.

INTRODUCTION

One of the principal factors limiting the performance time of gas
turbines used in current jet engines is the operating life of the
turbine blades. Improvement of blade life is therefore one of the
primary objectives of current gas-turbine research. Laboratory evalu-
ations of heat-resistant alloys have established such elevated-
temperature properties as stress rupture, creep, and fatigue strength
with the realization that one or a combination of all these properties
may define the life of a turbine blade. Before an alloy can be selected
for use as a blade material, however, a determination of the relative
importance of its various physical properties in defining blade life
is necessary.

Engine operation of a turbine blade can result in the following
types of failure:

    (1) Creep-rupture failure, resulting from centrifugal stress and
          temperatures

        (a) Creep failure, blade elongation in excess of defined
             limits

        (b) Stress-rupture failure, blade fracture before elongation
             exceeds defined limits

    (2) Fatigue failure, blade fracture due to alternating stresses

    (3) Thermal-shock failure, blade fracture due to thermal stresses
          resulting from temperature gradients

Failures can also result from the combined effects of several mechanisms,
for example, a fatigue failure originating at a crack produced by thermal
stresses. Another type of failure is that resulting from damage pro-
duced by other blade failures or failure of other engine components.
Because these failures occur as the result of extraordinary conditions,
they will not be considered in evaluating the performance of the blades.

A comparison of the results of blade performance in a gas turbine
with existing data from standard laboratory tests, when combined with
a determination of the mechanisms of blade failure, should yield a
basis for predicting blade life from the known high-temperature proper-
ties of an alloy.

As part of the over-all program to investigate heat-resistant alloys for use in turbojet engines, an investigation was conducted at the NACA Lewis laboratory to determine the high-temperature properties that define the turbine-blade life of a forged nickel-base alloy, Hastelloy B, and a precision case cobalt-base alloy, Stellite 21. The blades were alternately mounted in a 16-25-6 alloy rotor and operated under cyclic (simulated service) conditions in a J33-9 turbojet engine. At intervals during the engine operation, the turbine blades were measured to determine the amount of blade creep and inspected for evidence of failure or damage. Simultaneously with the engine operation high-temperature stress-to-rupture tests were conducted of specimens cut from the airfoil section of blades of each alloy to allow a comparison of the stress-rupture life of the blade with engine life. At the conclusion of operation, all blade and stress-rupture specimen failures were examined metallurgically to determine the nature of the origin of failure and the mechanism of failure propagation.

APPARATUS AND PROCEDURE

Turbine Blades

Fabrication history. -

Nominal chemical composition	Stellite 21 (reference 1)				Hastelloy B (manufacturer's data)			
	C	Cr	Mo	Ni	C	Mo	Fe	Ni
	0.20-.35	25.00-29.00	5.00-6.00	1.75-3.75	0.12 max.	26.0-30.0	4.0-7.0	Remainder
	Mn	Si	Fe	Co				
	1.00 max.	1.00 max.	2.00 max.	Remainder				

Fabrication	Precision cast	Forged
Heat treatment	None	2 hr at 1900° F, air-cooled 4 hr at 1500° F, air-cooled

Preinstallation inspection. -

Radiographic   All blades without flaws

Optical   Cross-sectional areas of several blades
comparator   measured; stress distributions calculated
                                by method described in reference 2

Installation (fig. 1). -

Rotor   16-25-6 alloy

Total number of blades   54

Blade positions   Alternated, with Stellite 21 blades odd
                                numbered and Hastelloy B blades even
                                numbered

Engine Operation

Engine. - (Engine, fuel, and engine instrumentation described in
reference 3)

Type   Turbojet

Designation   J33-9

Nominal thrust   4000 lb

Compressor   Dual-entry centrifugal

Combustion chambers   14

Operating cycle[a]. -

| Duration | | Rotor speed (rpm) | Gas temperature at exhaust-cone outlet (°F) |
(min)	(sec)		
4	30	4000 ± 50	1110 max.
0	15	Acceleration to 11,500	1450 ± 50
15	0	11,500 ± 50	1250 ± 20
0	15	Deceleration to 4000	1260 max.

[a]Cyclic operation was employed during this investigation to
    simulate the starting and shutdown conditions encountered
    in service.

Observations between engine operations. -

Measurement of blade and wheel elongation	Optical extensometer readings of an accuracy of $\pm$ 0.0001 in. between gage marks on two blades of each alloy and on the turbine wheel (see fig. 2)
Location and detection of blade cracks	Visual examination during engine shutdown and overhaul

Blade Specimen Stress-Rupture Tests

Loading system	Simple beam acting through system of knife edges
Furnace	Resistance type
Temperature control	Less than 5° F variation along specimen; average temperature variation $\pm$ 2° F
Specimens	Cut from center of blade airfoil section (see fig. 3)
Test conditions	Stress and temperature same as estimated at midpoint of blade during engine operation

Blade Examination after Testing

Determination of reduction in area of a blade of each alloy	Optical comparator
Examination of surface condition and fractures	Low-power microscope
Location of blade cracks	Fluorescent-oil examination
Hardness distribution along blades	Rockwell hardness tester
Microexamination of blade and stress-rupture specimen failures	Standard metallurgical equipment and procedures

RESULTS

Blade Stress Calculations

The results of the stress determinations based on the measured cross-sectional areas and 11,500 rpm for the two alloys Hastelloy B and Stellite 21 are plotted in figure 4. The stress curves are based on the average areas of six blades and an engine speed of 11,500 rpm.

Stress-Rupture Tests

The results of the rupture tests on the individual Hastelloy B and Stellite 21 specimens cut from blades are listed in table I. Microscopic examination of broken stress-rupture specimens indicated that the stress-rupture fractures were intercrystalline in both alloys (figs. 5 and 6).

Engine Operation

The results of engine operation and the blade examination after testing are listed chronologically in table II and the types of failure encountered are shown in figures 7 to 14.

Blade Elongation

The results of the elongation measurements on the blades are presented in figure 15. Figure 16 shows the time-elongation curves for the entire blades and for the gage sections with a total elongation at the conclusion of test of greater than 1 percent. There was no measureable elongation in the 16-25-6 alloy turbine rotor.

Blade Reduction in Area

The results of the reduction in area measurements of a Hastelloy B blade after 28.75 hours (115 cycles) of operation are shown in figure 17. These results are only qualitative inasmuch as they represent the change in area of a single blade compared with the average area of the Hastelloy B blades prior to operation. The measurements of the area of a Stellite 21 blade after operation did not indicate any measureable reduction in area.

Surface Condition and Oxide Coloring of

Blades and Blade Fractures

The Stellite 21 blade surfaces after 28.75 hours (115 cycles) of operation were coated with a thin dark-gray oxide and exhibited the "alligator skin" appearance characteristic of deformation in coarse-grained alloys, as described in reference 4. (See fig. 18.) The Hastelloy B blade surfaces were coated with a flaked dark-brown-to-purple oxide and exhibited a slight amount of oxide pitting. The fracture surfaces of all Hastelloy B blades were coated with a similar oxide pattern, a dark-gray oxide at the fracture origin that changed to a blue temper color as the fracture progressed across the blade. This same color pattern also existed on the fracture surface of Stellite 21 blade 25. The colorings of the fracture surfaces of Stellite 21 blades 1 and 3, however, were anomalous in that they were entirely a straw temper color.

Hardness Distribution along Blades after Operation

Typical hardness-distribution curves are shown in figures 19 and 20 for the Hastelloy B and Stellite 21 turbine blades, respectively, after 28.75 hours (115 cycles) of operation. Each point on these plots represents an average of three to five Rockwell-A hardness values. The hardness distributions in the blades that failed were generally the same as those in figure 19. These plots indicate that the maximum hardness occurs around the center of the airfoil section of the blades.

The hardness of as-received blades of these alloys ranged from a Rockwell-A of 63 to 65 for Stellite 21 and 55 to 57 for Hastelloy B. Manufacturer's data on these alloys indicate that age hardening occurs at 1500° F (the maximum blade temperature in the engine) and that the hardness changes observed at the point of maximum hardness are of the order of magnitude that would be expected for the times the blades were in operation.

DISCUSSION OF RESULTS

Blade Stress and Temperature

Before a complete analysis of the results of this investigation can be made the stress and temperature conditions to which the blades are subjected in the engine must be established. Earlier investigations of temperature distributions in turbine blades (reference 5) indicate that the maximum blade temperature occurs about at the middle

zone of the airfoil section of the blade or about 2 inches from the
top of the blade root. Although no temperature distributions are
available for the gas temperatures used in this investigation, measure-
ments at this laboratory of the maximum blade temperature at rated
speed indicate that for an average gas temperature of 1250° F (measured
at the exhaust-cone outlet) the maximum blade temperature ranges from
1450° to 1500° F depending on the operating characteristics of the
engine. The zone of maximum temperature is generally the failure zone
of the blades in this engine. From the average stress distributions
at rated speed for these alloys (fig. 4), the centrifugal stress at
the midpoint of the airfoil section of the Hastelloy B blades is
established at 25,000 pounds per square inch and the Stellite 21 blades
at 21,000 pounds per square inch. These stresses have been selected
as the critical stresses in the blades because they occur at the
estimated zone of blade failure and the point of maximum blade tempera-
ture. At the midpoint of the blade during operation, therefore, the
combined average stress and maximum temperature are 25,000 pounds per
square inch and 1500° F for Hastelloy B and 21,000 pounds per square
inch and 1500° F for Stellite 21.

Comparison of Laboratory and Engine Tests

     The results of the stress-rupture and engine tests of the
Hastelloy B and Stellite 21 blades are compared with available strength
data for these alloys in figure 20. All the blade failures are plotted
on this curve, although some of the failures apparently were not of the
stress-rupture type, to determine if stress rupture might have con-
tributed to initiating failure even though metallurgical examination
revealed no evidence of stress-rupture cracks. The design stress-
rupture data of the manufacturer for Hastelloy B at 1500° F, although
a heat treatment different from that of this investigation was used,
compare favorably with the results of the rupture tests on specimens
cut from blades. At a stress of 25,000 pounds per square inch, the
manufacturer's data indicate a rupture life of 12 hours; the blade
specimens had rupture lives ranging from 10.3 to 19.2 hours, or within
the range that might be expected from the manufacturer's data. In the
case of the alloy Stellite 21, the results of the blade-specimen
rupture tests fall within the stress-rupture band for the alloy. For
a maximum blade temperature of 1500° F, the minimum rupture life of
the Hastelloy B blades at the average stress of 25,000 pounds per
square inch would be 10.3 hours, the minimum rupture life of Stellite 21
blades at the average stress of 21,000 pounds per square inch would be
21 hours (minimum predicted by stress-rupture band).

     From the results of the engine operation, the first Hastelloy B
blade failure occurred in the trailing edge of blade 14 after
14.25 hours of operation or within the range predicted by the stress-

rupture tests (fig. 20). This failure, however, could not be classed
as a stress-rupture failure because unlike a rupture failure, it was
transcrystalline in its propagation and had a smooth fracture surface.
The failure started at a point on the blade above the zone of critical
stress and maximum temperature (fig. 7). From the nature of the
fracture, therefore, vibratory stresses were probably a principal
cause of this first failure. After 16.75 hours of operation, the
majority of the remaining Hastelloy B blades developed intercrystalline
leading-edge cracks characteristic of the stress-rupture failures of
the blade specimens. Inasmuch as this operating time was within the
stress-rupture failure times expected from operating conditions, these
cracks can be considered as evidence of the beginning of blade failure
by stress rupture. The distribution of these cracks along the leading
edge (fig. 11(a)) suggests that corrosion or localized hot zone along
the leading edge may have been partly responsible for their formation.
However, the correlation of the nature of the crack propagation and
the time of the crack formation with the results of the stress-rupture
tests on blade specimens indicates that other contributing causes such
as corrosion are of less importance. As the engine operation continued,
the remaining Hastelloy B blade fractures progressed from these leading-
edge cracks. The failures progressed by two mechanisms, fatigue and
stress rupture. Hastelloy B blades 4 and 34 (figs. 11(b) and 11(d))
fractured after 18.47 hours of (1.72 additional hr) operation as a
result of a condition favorable for fatigue fracture having been set up
by the leading-edge cracks. The vibratory stresses in the blades were
therefore merely propagating a failure originated by stress rupture.
In Hastelloy B blade 54 after 28.75 hours (12 additional hr) of opera-
tion, fracture occurred by the progression of the initial crack across
the blade continued by a stress rupture following an intercrystalline
path. Some of the original Hastelloy B blades were still in operation
at times in excess of the predicted rupture life, which would be
expected since a complete stress-rupture band for the alloy was unavail-
able, making the maximum blade life unknown. All but three of the
original 27 Hastelloy B blades, however, had cracked or fractured at
the conclusion of operation, indicating that failure had started in all
but three blades.

In the case of the Stellite 21 blades, the first blade failure
(blade 25) occurred after 16.75 hours, which is below the predicted
rupture life of 21 hours. Like the first Hastelloy B failure, the
fracture started at the trailing edge and was not of the character-
istic stress-rupture type inasmuch as it was transcrystalline in its
propagation and had smooth fracture facets. Also like the first
Hastelloy B failure, fracture started at a point above the zone of
critical stress and maximum temperature. As in the case of the first
Hastelloy B blade, therefore, vibratory stresses were largely responsi-
ble for this fracture. At this same time (16.75 hr), intercrystalline

cracking was detected in two Stellite 21 blades. The nature of
this cracking is characteristic of the beginning of failure by stress
rupture. Because the first cracked Stellite 21 blades were removed
from the engine, their exact life cannot be determined. However,
because seven of ten cracked Hastelloy B blades left in the engine at
the same time operated for 12 additional hours without failure, the
cracked Stellite 21 blades would probably have operated for the length
of time predicted by the rupture band before failing. At the conclusion
of operation, Stellite 21 blades 1 and 3 were fractured. Inasmuch as
blades 1 and 3 were close to the fractured blade 54 (fig. 14), failure
was probably caused by impact with the upper half of the fractured
blade. This mechanism of failure is corroborated by the following
facts: (1) The fracture surfaces were not of the stress-rupture or
fatigue type, and (2) the fracture surfaces were covered completely
with a light straw color indicating that the entire fracture occurred
at the same time and that the surfaces were exposed for only a very
short time. Because these failures are the result of extraordinary
causes, they will not be considered in evaluating the performance of
alloy Stellite 21. The only additional evidence of failure in
Stellite 21 at the conclusion of operation were the two additional
blades that had formed intergranular cracks of the stress-rupture type
after 28.75 hours of operation.

Blade Creep

The creep characteristics of the alloys during engine operation
can be determined by examining the elongation curves in figure 15.
In the case of the Hastelloy B blades, when cracking started at
16.75 hours the two blades that were measured had an elongation in the
gage section of greatest stretch of 5 percent. One measured blade,
Hastelloy B blade 54 (fig. 16(b)), shows some evidence of third-stage
creep at 16.75 hours but this change in the curve may be not signifi-
cant inasmuch as the same effect in blade 40 (fig. 16(a)) did not con-
tinue with further operation. After 28.75 hours of operation, blade 40,
the other measured blade, had a maximum elongation of 8 percent.
Blade 54 fractured so that no final elongation data could be determined.
Unfortunately no data were available in the literature for Hastelloy B
to check with the data for creep characteristics in the engine. The
zone of maximum elongation varied in the two scribed blades; in
blade 54 it was gage section 3 (from $1\frac{3}{8}$ to $1\frac{7}{8}$ in. from the top of the
root) and in blade 40 it was gage section 4 (from $1\frac{7}{8}$ to $2\frac{3}{8}$ in. from
the top of the root). These differences are probably the result of

dimensional differences between the blades that produced different stress distributions. The results of the blade-hardness and reduction-in-area measurements of the Hastelloy B blades both indicate that the elongation measurements are fairly reliable in defining the zone of maximum stress and temperature effect in the blades.

In the case of the Stellite 21 blades (figs. 16(c) and 16(d)), at the time that first cracks were noted (after 16.75 hr of operation) maximum elongations of around 2 percent existed in gage section 4 on the blades. This gage section, which is from $1\frac{7}{8}$ to $2\frac{3}{8}$ inches from the top of the blade root, exhibited the highest elongation in both scribed blades. The curves in figures 16(c) and 16(d) also show a slight change in slope at about 2-percent elongation. Because first cracks were also noted at 16.75 hours, this time probably marks the initiation of third-stage creep. Although the sensitivity of the method of creep measurement is probably not high enough to make this change in slope of the time-elongation curves significant, the results are somewhat confirmed by the work of other investigators. The data in reference 7 indicate that Stellite 21 when rupture-tested at a temperature of 1500° F and a stress of 20,000 pounds per square inch will enter third-stage creep at elongations of about 2 to 3 percent. The time-elongation curves for both the Stellite 21 and Hastelloy B blades also illustrate the unreliability of total blade-elongation measurements as a means of predicting the creep characteristics of an alloy during service operation. The results plotted in figure 16 indicate that the percentage elongation in localized zones in the blade can be one to three times the percentage elongation of the entire blade.

Prediction of Blade Life

The results of the blade-operation and blade-elongation measurements indicate that the engine life of alloys Stellite 21 and Hastelloy B as turbine blades in the engine used in this investigation can be defined to some extent by their creep and rupture properties. Although the number of fractured blades of each sample was small both alloys had a number of cracked blades. In the case of the shorter-lived Hastelloy B blades, 88 percent of the blades were either fractured or cracked. In the case of the longer-lived Stellite 21 blades, 15 percent of the blades were cracked. These first cracks serve as the probable nuclei of fatigue failures and although the rupture life of the alloy extends beyond this point the probability of failure has been greatly increased by these cracks and further operation of these blades is undesirable. The defining point in the life of these blades was therefore the time of initiation of stress-rupture cracks. The initiating of this first cracking

is probably very closely associated with the beginning of third-stage
creep in the blades. The limited number of failures and the fact that
the elongation of only two blades of each alloy was determined prevent
a more exact prediction of the relation between creep, stress-rupture
properties, and blade life. It should be noted that the first failures
of both the Stellite 21 and Hastelloy B blades were anomalous in the
sense that they were not of the stress-rupture type, although the
Hastelloy B blade did fail within the time predicted by stress-rupture
tests. The similarity of these two failures is apparently significant.
Both were probably the result of vibratory stresses superimposed on
the centrifugal stresses. These blades represented only 3.7 percent
of each blade sample, however, and therefore were not characteristic
of all blades of the alloys. Any of the following factors could have
caused these blades to become susceptible to vibratory-stress failure:
(1) flaws in blades not detectable by regular inspection; (2) undetect-
able surface damage; and (3) unusual vibratory stresses. The cause of
these failures should be determined so that they can be eliminated to
allow alloys to perform as turbine blades to their full life as pre-
dicted by their elevated-temperature stress-rupture and creep properties.

It should be emphasized that the results of this investigation were
obtained in a specific turbojet engine. With changes in the design of
this engine or in other types of engine, operating conditions may pro-
duce different results so that a prediction of material blade life may
depend on properties other than those determined in this investigation.

SUMMARY OF RESULTS

The following results were obtained from a cyclic evaluation of
the alloys Stellite 21 and Hastelloy B as turbine blades in a J33-9
engine at a rotor speed of 11,500 rpm and a gas temperature at the
exhaust-cone outlet of 1250° F. For these operating conditions, the
estimated conditions in the zone of blade failure were a maximum
temperature of 1500° F and a stress of 25,000 pounds per square inch
for the Hastelloy B blades and a stress of 21,000 pounds per square
inch for the Stellite 21 blades.

1. The expected minimum life of the turbine blades at the con-
ditions in the zone of blade failure on the basis of stress-rupture
tests on specimens cut from turbine blades was 10.3 hours for
Hastelloy B and 21 hours for Stellite 21.

2. The first blade failure of the Hastelloy B blades occurred
after 14.25 hours (57 cycles). The first Stellite 21 blade failure
occurred after 16.75 hours (67 cycles) of operation. Both failures
started at the trailing edges above the zone of maximum temperature
and high stress and were probably the result of excessive vibratory
stresses.

3. Intercrystalline cracking of the stress-rupture type was detected in both alloys after 16.75 hours (67 cycles).

4. Additional failures occurred in Hastelloy B blades after 18.47 hours (< 74 cycles) and 28.75 hours (115 cycles). These resulted from the propagation of the previously formed intercrystalline cracks by both fatigue and stress-rupture mechanism. At the conclusion of 28.75 hours of operation, 24 of the original 27 Hastelloy B blades, which had not failed, had stress-rupture-type cracks.

5. No additional Stellite 21 failures occurred up to 28.75 hours (115 cycles) except two blades that were fractured by impact with the fractured half of a Hastelloy B blade. At the conclusion of 28.75 hours of operation, four of the original 27 Stellite 21 blades had stress-rupture-type cracks.

Lewis Flight Propulsion Laboratory,
    National Advisory Committee for Aeronautics,
        Cleveland, Ohio.

REFERENCES

1. Anon.: Alloy Castings, Precision Investment, Corrosion and Heat Resistant. AMS 5385, SAE, Sept. 1, 1947.

2. Kemp, Richard H., and Morgan, William C.: Analytical Investigation of Distribution of Centrifugal Stresses and Their Relation to Limiting Operating Temperatures in Gas-Turbine Blades. NACA RM E7L05, 1948.

3. Farmer, J. Elmo, Darmara, F. N., and Poulson, Francis, D.: Cyclic Engine Test of Cast Vitallium Turbine Buckets - I. NACA RM E7J23, 1948.

4. Yaker, Charles, and Garrett, Floyd B.: Cyclic Engine Operation of Cast Vitallium Turbine Blades at an Exhaust-Cone Gas Temperature of 1440 ± 20° F. NACA RM E9G13, 1949.

5. Farmer, J. Elmo: Relation of Nozzle-Blade and Turbine-Bucket Temperatures to Gas Temperatures in a Turbojet Engine. NACA RM E7L12, 1948.

6. Grant, Nicholas J.: The Cobalt-Chromium J Alloy at 1350 to 1800° F. Trans. A.S.M., vol XL, 1948, pp. 585-610; written discussion by F. S. Badger, pp. 611-613.

7. Cross, Howard C.: Progress Report on Heat Resisting Metals for Gas Turbine Parts (N-102). OSRD No. 1871, Serial No. M-147, NDRC, Oct. 1, 1943.

TABLE I - STRESS-RUPTURE LIFE OF BLADE SPECIMENS

AT TEMPERATURE OF 1500° F

Stress (lb/sq in.)	Rupture life (hr)	
	Hastelloy B	Stellite 21
20,000	----	55.0
20,000	----	43.0
20,000	----	55.0
20,000	----	38.2
22,000	----	35.0
22,000	----	19.3
22,000	----	20.4
22,000	----	21.3
30,000	----	12.0
30,000	----	6.0
25,000	15.4	----
25,000	12.1	----
25,000	10.3	----
25,000	18.4	----
25,000	19.2	----

NACA

TABLE II – RESULTS OF ENGINE OPERATION AND POST-OPERATION INSPECTION OF HASTELLOY B AND STELLITE 21

Alloy	Blade	Time at rated speed (hr)	Origin of failure[a]	Turbine blades		Apparent cause of failure[b]
				Description of failure surface	Failure propagation	
Hastelloy B	14[c]	14.25	Trailing-edge crack	Partly smooth and partly rough appearance (see fig. 7)	Transcrystalline (fig. 8)	Vibratory stresses superimposed on centrifugal stress (fatigue)
Stellite 21	25[c]	16.75	Trailing-edge fracture	Fracture path at angle to horizontal. Fracture started with zone with smooth crystalline facets then changed to zone of rough surface (fig. 9(a))	Transcrystalline (fig. 10)	Vibratory stresses superimposed on centrifugal stress (fatigue)
Hastelloy B	4 6 8[c] 10[c] 12[c] 16 18 20[c] 22 30[c] 32[c] 34 36[c] 38[c] 46[c] 48 50[c] 52 54	16.75	Leading-edge cracks (for example, fig. 11(a))		Intercrystalline (fig. 12)	Centrifugal stress (stress rupture)
Stellite 21	17[c] 21[c]	16.75	Center cracks (away from edges)		Intercrystalline	Centrifugal stress (stress rupture)
Hastelloy B	4[c]	18.47	Leading-edge fractured[d]	Fracture started normal to edge from point where crack was observed then changed direction and moved at angle with horizontal. The surface in flat portion of fracture has concentric-ring markings typical of fatigue failure. The remaining surface has coarse appearance (figs. 11(b) and 11(c)).	Intercrystalline changing to transcrystalline (fig. 13)	Centrifugal stress at origin, fracture then propagated to vibratory stresses (stress rupture to fatigue)
Hastelloy B	34[c]	18.47	Extension of leading-edge crack (crack only)	Same as start of fracture in blade 4 (fig. 11(d))	Intercrystalline changing to transcrystalline (fig. 13)	Same as preceding blade 4
Hastelloy B	54[c]	28.75[e]	Leading-edge fractured[d]	Fracture path at angle to horizontal from point where crack was observed. Entire surface has coarse appearance (fig. 11(e)).	Intercrystalline	Centrifugal stress (stress rupture)
Hastelloy B	2 24 26 28	28.75	Leading-edge cracks		Intercrystalline (fig. 12)	Centrifugal stress (stress rupture)
Stellite 21	1 3	28.75	Fracture origin not determinable	Irregular fracture surface having coarse appearance (figs. 9(b) and 9(c))	Transcrystalline	Impact with failure fragments suggested by close proximity of failures as shown in fig. 14
Stellite 21	33 45	28.75	Center cracks (away from edges)		Intercrystalline	Centrifugal stress (stress rupture)

a Based on results of prefailure inspection and oxide coloring.
b Based on failure propagation in stress-rupture tests and appearance of fracture surface.
c Blade replaced with new blade.
d Failures at points of previously noted cracks.
e Test was concluded at this time because of severe damage to remaining blades in rotor.
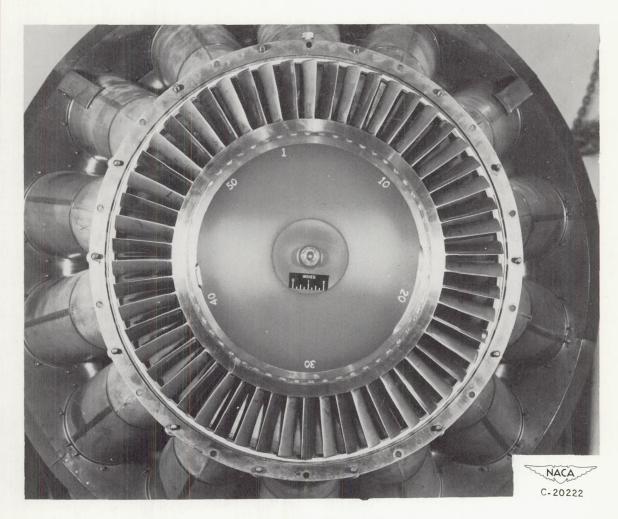
Figure 1. - Turbine rotor of Timken alloy before operation, alternately bladed with Hastelloy B and Stellite 21 turbine blades.
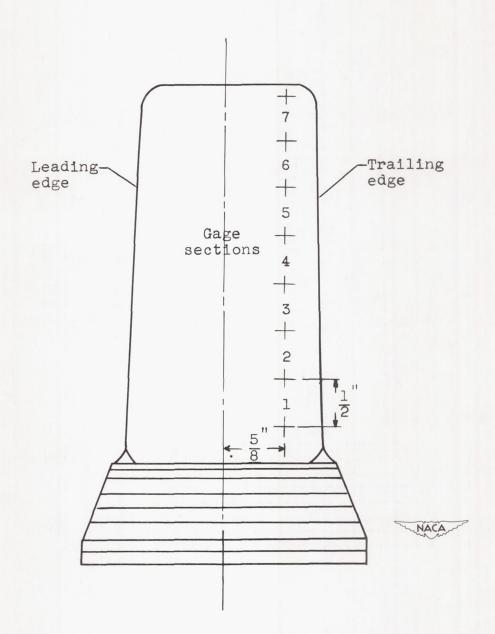
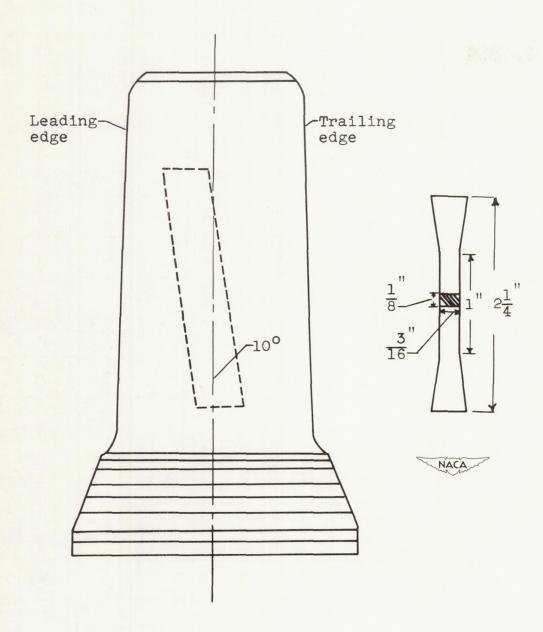Figure 2. - Location of scribe marks on convex side of turbine blade for measurement of elongation.

Figure 3. - Blade stress-rupture specimen and zone
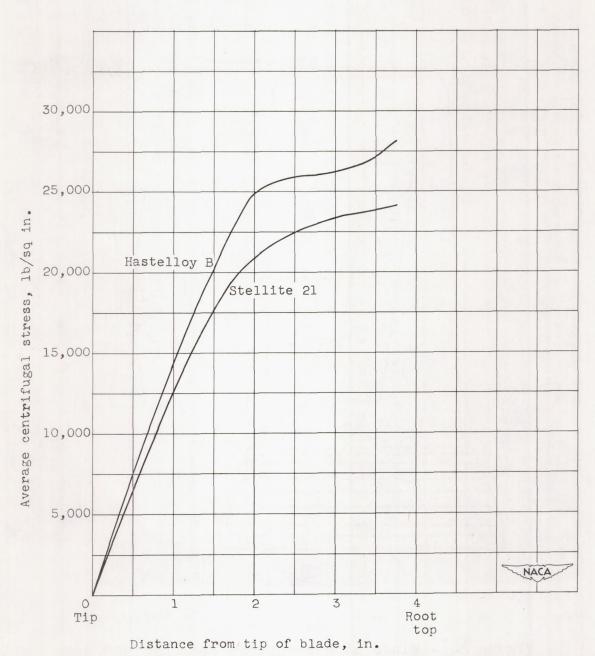from which specimen is machined.

Figure 4. – Average centrifugal stress distributions in Hastelloy B and Stellite 21 turbine blades at rotor speed of 11,500 rpm.
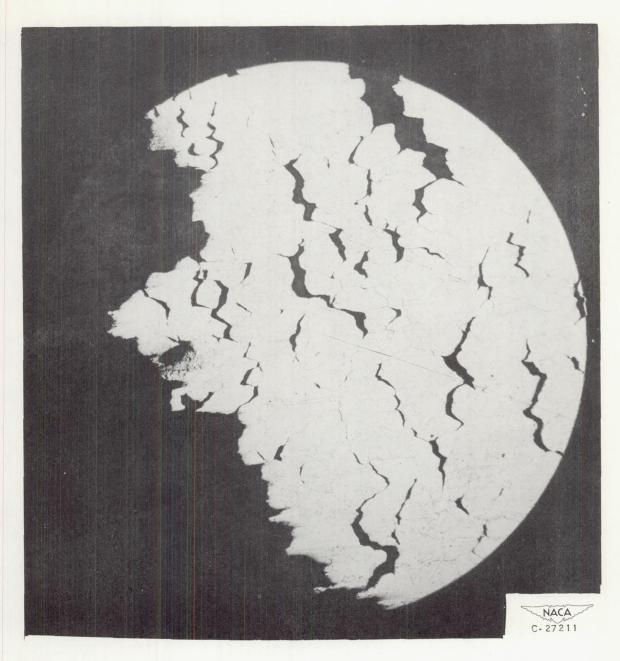
Figure 5. - Intercrystalline fracture in Hastelloy B stress-rupture specimen. Etched in solution of aqua regia in glycerine. X50.
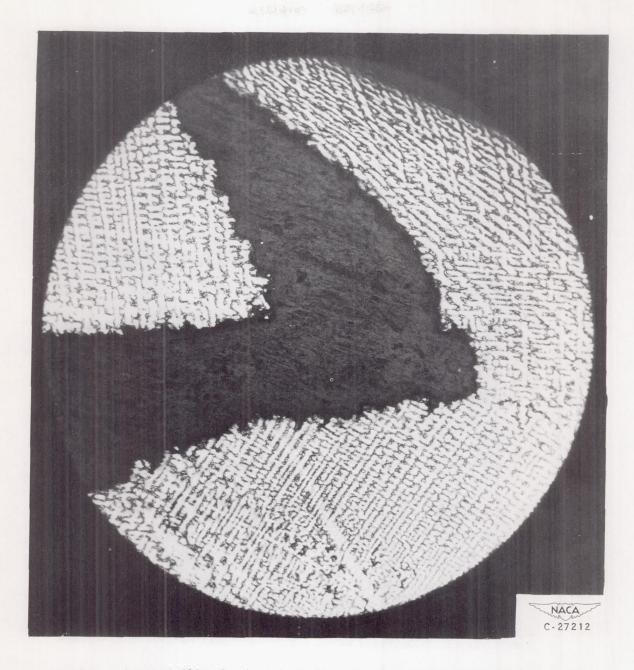
Figure 6. - Intercrystalline fracture in Stellite 21 stress-rupture specimen. Electro-
lytically etched in solution of 10-percent nitric acid and 10-percent ethylene glycol
in ethyl alcohol. X50.
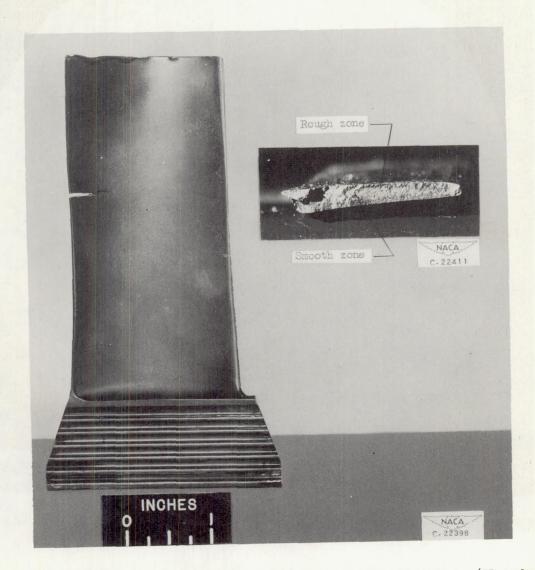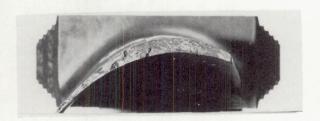
Figure 7. - Trailing-edge crack in Hastelloy B blade 14 after 14.25 hours (57 cycles)
of operation. (Fracture surface of crack at X5 shown in inset.)

Figure 8. - Transcrystalline trailing-edge crack in Hastelloy B blade 14 after 14.25 hours (57 cycles) of operation. Etchant, aqua regia in glycerine. X250.
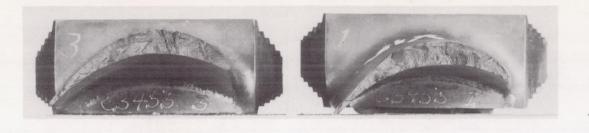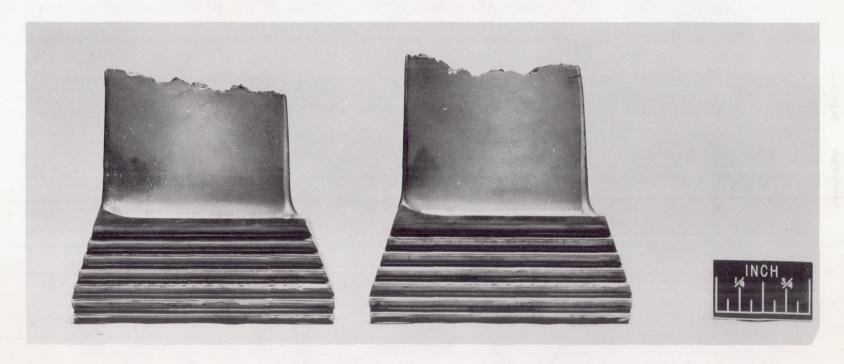
(a) Blade 25 fractured after 16.75 hours (67 cycles) of operation.

Figure 9. - Fractured Stellite 21 blades.

NACA
C-27215

(b) Blade 3 fractured after 28.75 hours (115 cycles)
of operation.

(c) Blade 1 fractured after 28.75 hours (115 cycles)
of operation.

Figure 9.-Concluded. Fractured Stellite 21 blades.

Trailing edge
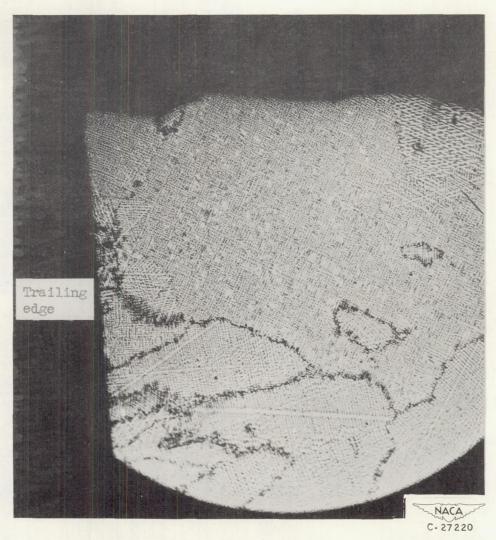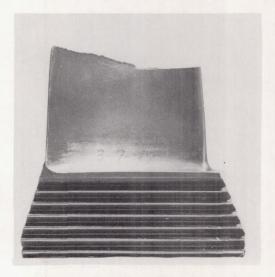
Figure 10. - Transcrystalline path in Stellite 21 fracture blade 25 after 16.75 hours (67 cycles) of operation. Electrolytically etched in 10 percent nitric acid and 10 percent ethylene glycol. X50.
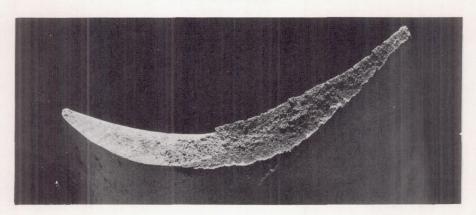
(a) Blade 52 after 28.75 hours (115 cycles) of operation.

(b) Blade 3 fractured after 28.75 hours (115 cycles) of operation.

(c) Fracture surface of blade 4 (fig. 11(b)). X2.

Figure 11. - Fractured and cracked Hastelloy B blades.

C-27216
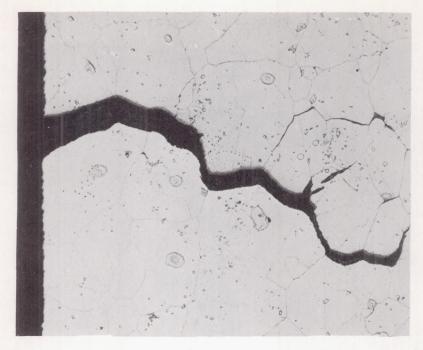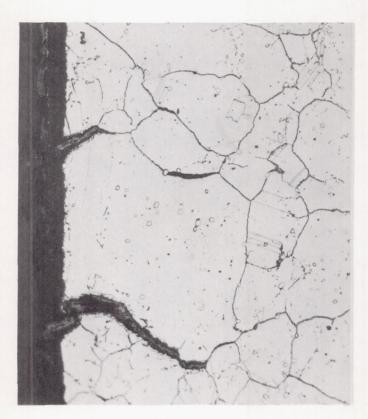
(d) Blade 34 after 18.47 hours (74 cycles)   (e) Blade 54 fractured after 28.75 hours
of operation.   (115 cycles) of operation.

Figure 11. - Concluded. Fractured and cracked Hastelloy B blades.

(a) X100.
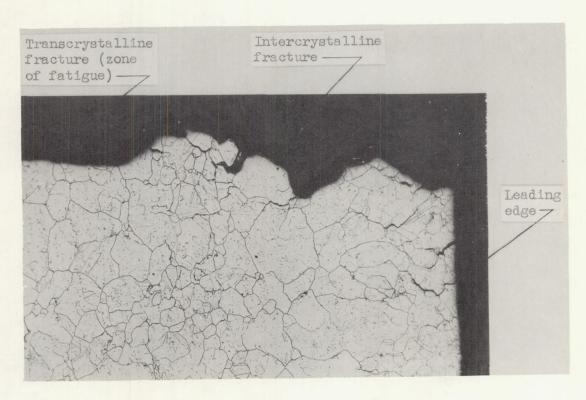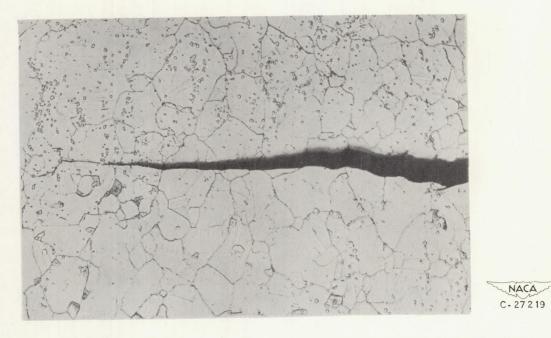
(b) X250.

Figure 12. - Typical intercrystalline leading-edge cracks in Hastelloy B blades. Etchant, aqua regia in glycerine.

(a) Failure path from leading edge of fractured blade 4. X50.

(b) Transcrystalline failure path in zone of fatigue of cracked blade 34. X100.

Figure 13.-Failure progression in Hastelloy B blades. Etchant, aqua regia in glycerine.
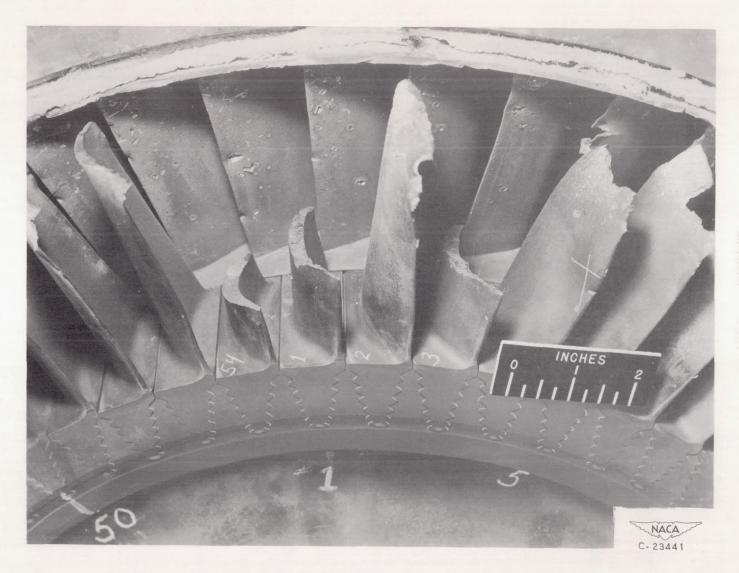
Figure 14. - Fractured blades at conclusion of operation.

(a) Hastelloy B blade 40.
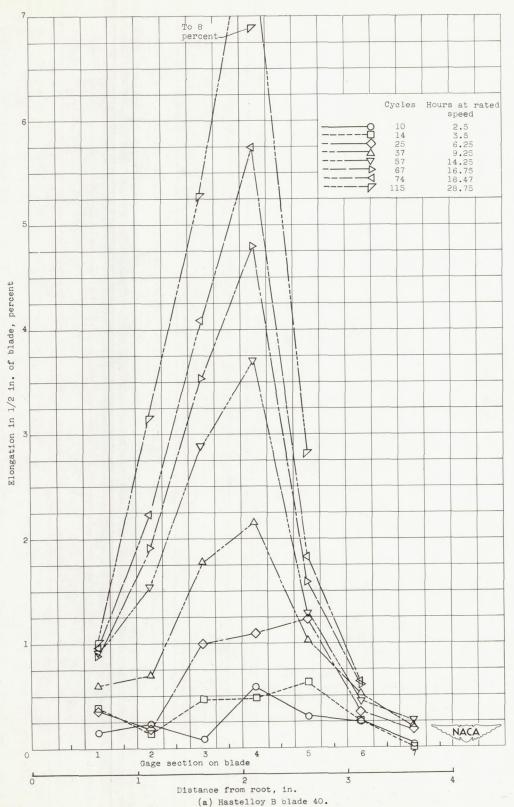
Figure 15. – Elongation distributions along turbine blades.

(b) Hastelloy B blade 54.
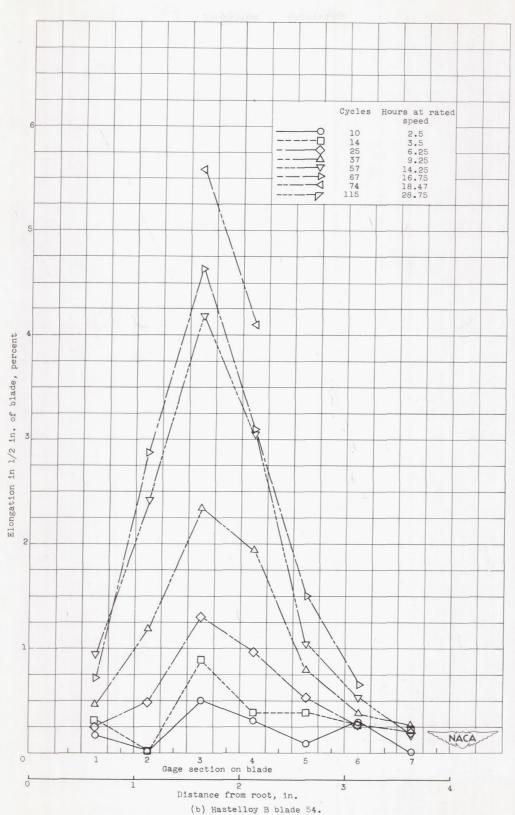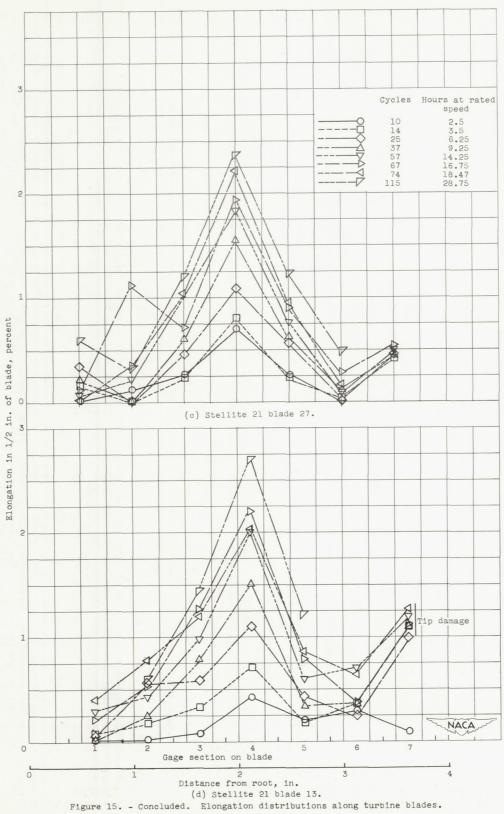
Figure 15. - Continued. Elongation distributions along turbine blades.

(c) Stellite 21 blade 27.

(d) Stellite 21 blade 13.

Figure 15. - Concluded. Elongation distributions along turbine blades.

(a) Hastelloy B blade 40.
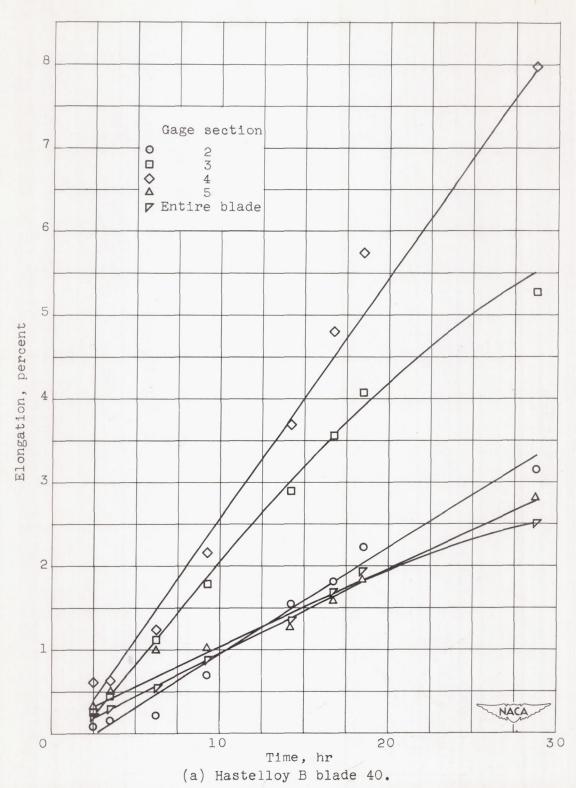
Figure 16. - Blade elongation during turbine operation for those sections having greater than 1 percent elongation.

(b) Hastelloy B blade 54.
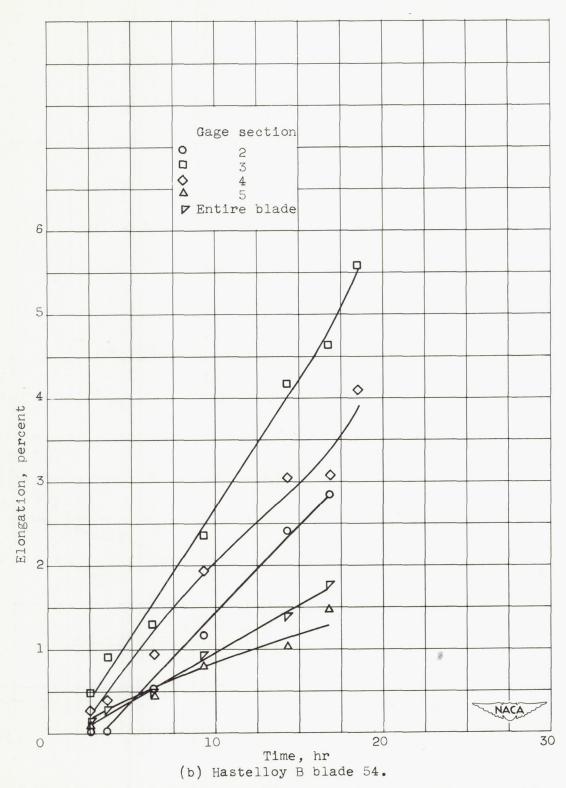
Figure 16. - Continued. Blade elongation during turbine operation
for those sections having greater than 1 percent elongation.

(c) Stellite 21 blade 27.
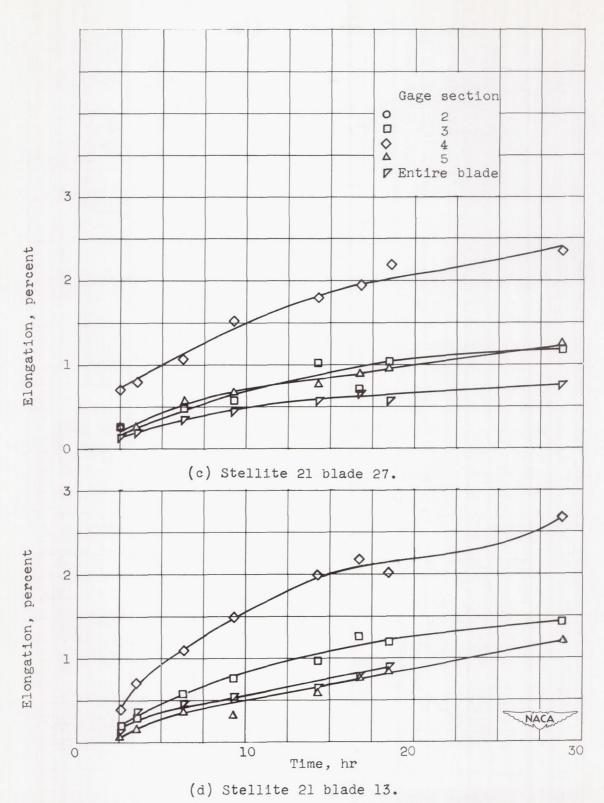
(d) Stellite 21 blade 13.

Figure 16. - Concluded. Blade elongation during turbine operation
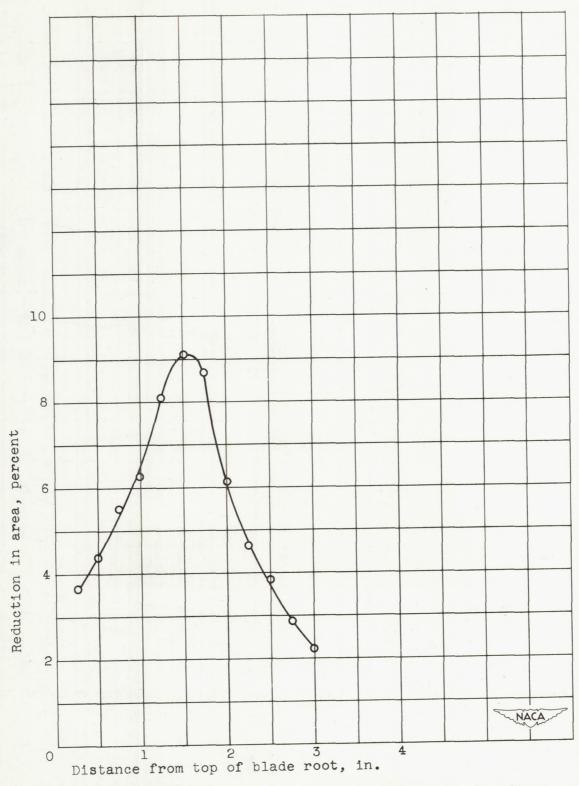for those sections having greater than 1 percent elongation.

Figure 17. - Reduction in area in Hastelloy B blade after
28.75 hours (115 cycles) of operation.

Figure 18. - Surface condition of Stellite 21 blade after 28.75 hours (115 cycles) of operation.
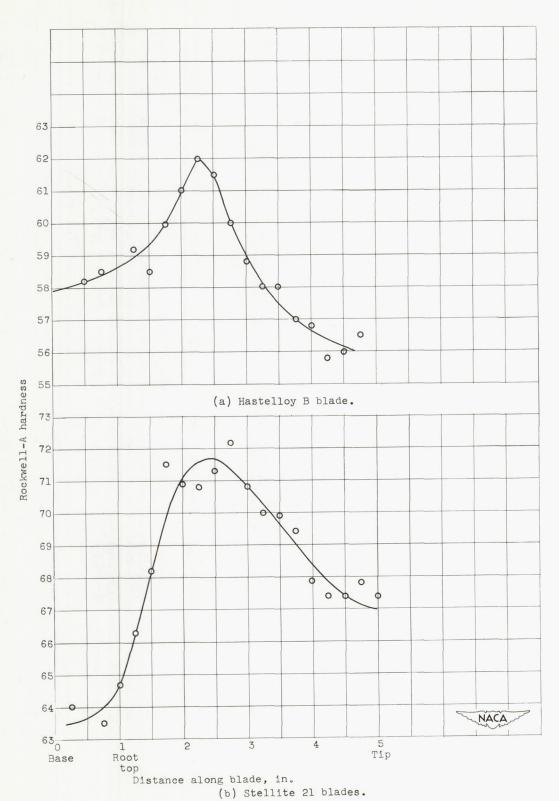
(a) Hastelloy B blade.

(b) Stellite 21 blades.

Figure 19. - Hardness distribution for blade after 28.75 hours (115 cycles) of operation.

(a) Hastelloy B blades.

(b) Stellite 21 blades.

Figure 20. - Comparison of stress-rupture properties and engine blade life at temperature of 1500° F for alloys Hastelloy B and Stellite 21.